J Mater Sci (2007) 42:2830–2836
DOI 10.1007/s10853-006-1364-1

Kinetics of the $\gamma \rightarrow \alpha$-alumina phase transformation by quantitative X-ray diffraction

Maria Iaponeide Fernandes Macêdo · Celso Aparecido Bertran · Carla Cristiane Osawa

Received: 9 January 2006 / Accepted: 27 February 2006 / Published online: 13 January 2007

Abstract This work reports the kinetics of α-alumina transformation from γ-alumina, prepared by the sol-gel method from a solution of saturated aluminum nitrate and urea. The γ-alumina phase transformed directly into α-alumina at 750, 800, 850 and 900 °C, without any intermediate phases, such as θ- or δ-alumina. The kinetics of $\gamma \rightarrow \alpha$-alumina phase transformation was monitored by determination of α-alumina fraction formed through quantitative X-ray diffraction (XRD), with calcium fluoride added as an internal standard. The crystallised fractions of α-alumina increased sigmoidally with time, indicating that the $\gamma \rightarrow \alpha$-alumina phase transformation had a nucleation and growth mechanism. The kinetic parameters for this transformation were determined through the Kolmogorov–Johnson–Mehl–Avrami (KJMA) model and the Arrhenius' law. The apparent activation energy, the Avrami exponent, n, and the $t_{0.75}/t_{0.25}$ ratio determined for the transformation were, respectively, of (201 ± 4) kJ mol_{-1} (2.1 ± 0.2) and (2.1 ± 0.1). The apparent activation energy is lower than the values previously reported for the $\gamma \rightarrow \alpha$-alumina transformation, as a consequence of the high surface area (425 m^2/g) of γ-alumina. The $t_{0.75}/t_{0.25}$ ratio of (2.1 ± 0.1) suggested that the α-alumina growth was plate-like, which was confirmed by the SEM micrograph of α-alumina.

M. I. F. Macêdo
Chemistry Institute, Federal University of Rio de Janeiro (UFRJ), Centro de Tecnologia, Bloco A, Cidade Universitária, CEP 21945-970 Rio de Janeiro, RJ, Brazil

C. A. Bertran (✉) · C. C. Osawa
Chemistry Institute, State University of Campinas (UNICAMP), P.O. Box 6154, 13084-871 Campinas, SP, Brazil
e-mail: bertran@iqm.unicamp.br

Introduction

Aluminum oxide can exist in a large variety of crystallographic forms. For instance, γ-, δ- and θ-alumina, called transition aluminas, are metastable forms of aluminum oxide and are widely used as adsorbents, supports for catalysts, coatings and soft abrasives [1–3], while α-alumina is the most stable Al_2O_3 polymorph and is usually crystallized at high temperatures [4–7].

The study of alumina transformation kinetics is very important because it is generally desirable that the phase transformations occur quickly at low temperatures to minimize the activation energy for the process in the manufacture of the α-alumina powders. Consequently, a search for new ways to decrease the transformation temperature is of great interest.

Depending on the synthesizing route employed, aluminum oxide can undergo several transformations under heating, from transition aluminas to the α-alumina phase [2, 8-12]. The sequence of phases formed and the temperatures required for each phase transformation depend either on the origin or on the granulometry of the alumina precursors. The presence of impurities may also affect the temperature required for the phase transformations.

The $\gamma \rightarrow \alpha$-alumina phase transformation requires a rearrangement of cations and anions, as their structures are different. γ-Alumina has a cation

deficient spinel structure, consisting of cubic close-packed oxygen anion layers with the aluminum cations both in octahedral and tetrahedral sites, while α-alumina has the corundum structure, which consists of hexagonal close-packed oxygen anion layers with aluminum present only in octahedral sites. Several authors reported that the approximate temperatures required for the phase transformations in the crystallisation sequence are: boehmite $\rightarrow$ γ (300 °C); $\gamma \rightarrow$ δ (850 °C); $\delta \rightarrow$ θ (1100 °C) and $\theta \rightarrow$ α (≥1200 °C) [5, 7, 13–19].

Although several authors have studied the kinetics and the apparent activation energies for the transformation of transition aluminas (γ-, δ- or θ-) to α-alumina [7, 12, 20–22], there are contradictory data reported in literature. An apparent activation energy value in the range of 210–600 kJ mol^{-1} was reported for the $\gamma \rightarrow$ α-alumina transformation [23]. Wilson and McConnel [12] found an apparent activation energy of 395 kJ mol^{-1} for α-alumina crystallisation; Shelleman et al. [20] and McArdle and Messing [22] found apparent activation energies for the $\gamma \rightarrow$ α-alumina transformation, respectively, of 431 and 578 kJ mol^{-1}, while Nishio and Fujiki [21] found them in the range of 408–473 kJ mol^{-1}.

The discrepancy between these results may be attributed to the methods employed for the α-alumina synthesis and the effects of several parameters such as the different starting materials used, presence of impurities, the degree of alumina defects, mechanical and thermal pretreatments, presence of additives, etc. [7, 19, 23].

In the present work, kinetic parameters such as k (rate constant), n (Avrami exponent) and the apparent activation energy for the $\gamma \rightarrow$ α-alumina transformation were determined by quantitative X-ray diffraction (XRD) using the Kolmogorov–Johnson–Mehl–Avrami (KJMA) model and the Arrhenius' law. The γ-alumina phase was characterised by ^{27}Al magic angle spinning nuclear magnetic resonance (^{27}Al MAS-NMR), Fourier transform infrared (FTIR) spectroscopy, surface area and X-ray Diffraction (XRD) while the α-alumina phase was characterised by XRD and the morphology of the growing α-alumina crystal was verified by scanning electron microscopy (SEM).

Experimental procedures

Sample preparations

Nonahydrated aluminum nitrate ($Al(NO_3)_3{\cdot}9H_2O$) (Reagen, analytical grade) was dissolved in deionized water at 22 °C under magnetic stirring near its saturation point (ca. 70 g/100 mL H_2O). Urea (CON_2H_4) (Reagen, analytical grade) was added until the molar ratio Al^{3+}: urea reached 1: 13 (ca. 152 g urea/100 mL H_2O). The solution was kept in a 22 °C water bath for 1 h and then passed through a 0.45 μm Millipore filter [24].

The aluminum/urea solution was heated at 90 °C for ~12 h. The initial solution pH, around 2.0, gradually increased, rose steeply from 3 to 6, and then more gradually until it reached a constant value of 8.0, and formed a transparent gel [24].

The freshly prepared alumina gel was dried at 90 °C and pre-calcined by placing it directly in a furnace (Robertshaw Division Pyrotec) operating at 300 °C for 25 min to eliminate the remaining urea and nitrate and result in a xerogel.

In order to determine the kinetic parameters, the xerogel was heated in the same furnace at the temperatures previously established between 750 and 900 °C for several heating periods.

Characterisation

The xerogel was characterised by FTIR spectroscopy, high-resolution solid-state ^{27}Al magic-angle spinning nuclear magnetic resonance and by measurement of its surface area.

The FTIR spectrum of the sample, prepared by the pellet method with IR-grade KBr in a 1:100 (w:w) ratio pressed as a transparent pellet by an axial method, was recorded in an FTIR spectrometer (Bomen/MB Series, B 100 model) in the wavenumber range of 4000–400 cm^{-1}, with 64 scans and a spectral resolution of 4 cm^{-1}.

High-resolution solid state ^{27}Al magic-angle spinning nuclear magnetic resonance (^{27}Al-MAS NMR) spectrum was performed at room temperature with a Bruker AC 300/P spectrometer with 4 mm zirconia rotors spinning the sample at the magic angle (54°44′) at 4 kHz, a pulse width of 4 μs and a recycle time of 1 s. Chemical shifts were expressed in ppm, relative to a standard reference of 1.0 mol/L aqueous aluminum nitrate solution (0 ppm).

The surface area of the xerogel was measured in a sorption analyzer, Micromeritics Instrument Corporation Flow Sorb 2300, with N_2 as the adsorbed gas, using the Brunauer-Emmett-Teller (B.E.T.) method.

The morphology of the xerogel sample after heating at 800 °C for 21,600 min was determined with a JEOL microscope, JSMT-300 model. Before scanning, this sample was chemically etched with 2 mol/L HCl (Reagen, analytical grade) for 10 min to eliminate

residues of the amorphous matrix, washed with isopropyl alcohol (Reagen, analytical grade) and dried. The powder was dispersed in a small quantity of a fused mixture of 60% camphor and 40% naphthalene (Reagen, analytical grade). A drop of this mixture was placed on a microscope sample holder and the volatile organic substances were sublimated under vacuum. The resulting sample was coated with gold by the sputtering method and analysed in the microscope.

Isothermal kinetic measurements

Samples of approximately 1 g of the xerogel were heated at temperatures between 750 and 900 °C for suitable time periods between 3 and 40,500 min. For each time, one sample of the xerogel was used. A chromel-alumel thermocouple was placed directly above the sample at the centerpoint of the furnace to monitor the sample temperature, which was stable within ±2 °C. The extent of α-alumina transformation was determined by quantitative XRD of the isothermally heated powders. These powders were mixed with CaF_2 (Merck, analytical grade), employed as an internal standard [20, 25, 26] in a ratio of 30% (w/w), before the acquisition of the diffractograms.

The diffractograms were obtained with a XD-3A Shimadzu diffractometer, composed of a model VG-108R goniometer and A-40 Cu X-ray generating tube, operating with CuKα radiation, 35 kV and 25 mA, with scanning rate of 1°/min between 20 and 70 ° (2θ).

Results and discussion

Xerogel characterisation

To characterise the xerogel, the alumina gel heated at 300 °C for 25 min was analysed by FTIR, ^{27}Al MAS-NMR and XRD. Figures 1–3 show these characterisation results.

The ^{27}Al MAS-NMR spectrum of the xerogel (Fig. 1) presents peaks centered at 5 and 65 ppm, assigned, respectively, to the aluminum ions in octahedral and tetrahedral environments, with predominance of aluminum ions in octahedral sites, which is characteristic of γ-alumina [17, 24, 27–30]. The FTIR spectrum of the xerogel (Fig. 2) shows bands centered at ~600 and ~800 cm^{-1}, assigned to the Al–O bonding vibration, respectively, in tetrahedral and octahedral environments, which suggests that the xerogel was γ-alumina [24, 30]. The band located at ~3440 cm^{-1} is attributed to the O–H stretching vibration and the band at ~1640 cm^{-1}, to the H–O–H symmetric stretching vibration of adsorbed water molecules.

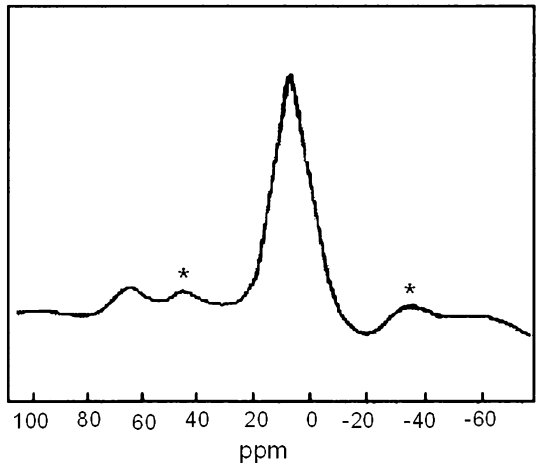

Fig. 1 ^{27}Al MAS-NMR spectrum of the gel heated at 300 °C for 25 min (xerogel). (*) spinning side band

The diffractogram of the xerogel (Fig. 3) presents low-intense and broad bands centered at 37, 46 and 67° (2θ-CuKα), which permits to characterize the xerogel as γ-alumina (JCPDS file card number 47-1308). The diffractogram pattern also indicates that the material is poorly crystalline.

The surface area determination showed that the γ-alumina had a high specific surface area of 425 m^2/g.

Kinetic results

Figure 4 shows the quantitative X-ray diffraction patterns of the xerogel heated at 750, 800, 850 and 900 °C for several heating periods, with CaF_2 added after heating as an internal standard. The peaks present in the diffractogram of the xerogel heated at 750 °C for 20,160 min corresponds to α-alumina (JCPDS file card number 10-173). Intensities of the peaks increased with temperature and heating periods and the positions and relative intensities of the peaks from the xerogel heated at 900 °C for 1500 min completely agree with the ones assigned to α-alumina. The sum of the integrated most intense peaks of α-alumina at 35.2°, 43.2° and 57.5° (CuKα-2θ) and the sum of the integrated most intense peaks of calcium fluoride at 28.1° and 46.9° (CuKα-2θ) were determined and their ratios were compared against a standard α-alumina/CaF_2 calibration curve [20, 26]. The sums of the integrated intensities of the most intense diffraction peaks were used to minimize preferential orientations of the crystalline planes. Errors were estimated as 2% (w/w), based on repeated measurements under the same conditions.

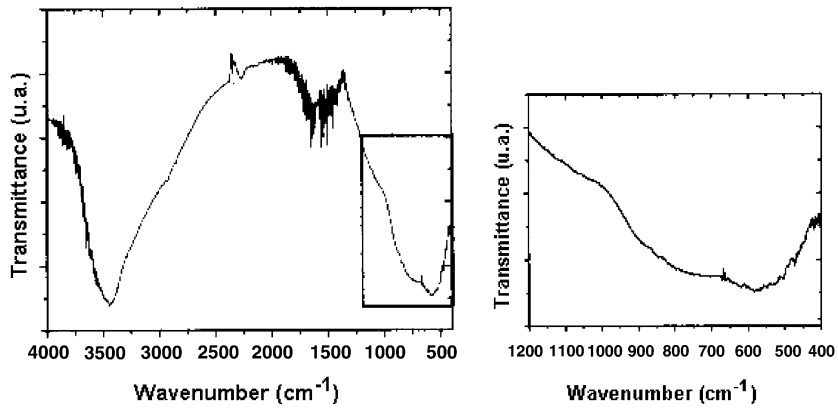

Fig. 2 FTIR spectrum of the gel heated at 300 °C for 25 min (xerogel)

Figure 5 shows the normalized isotherms performed at 750, 800, 850 and 900 °C for α-alumina crystallization obtained from the quantitative X-ray diffraction data. The crystallised fractions of α-alumina increase sigmoidally with time, indicating that the $\gamma \rightarrow \alpha$-alumina transformation can be considered a nucleation and growth mechanism and that the phase transformation data can be described by the Kolmogorov–Johnson–Mehl–Avrami (KJMA) kinetic equation (Eq. 1) [31–35].

$$x = 1 - \exp(-kt^n), \quad (1)$$

Where x is the crystallised fraction of α-alumina; t is the effective time; n is the Avrami exponent and k is the rate constant, which depends on the nucleation and growth rates.

For determination of the k and n values, each kinetic curve (Fig. 5) fitted Eq. 1, using Origin 6.1 software with Simplex and the sigmoidal Sweibull 1 curve option taken in successive steps of 10 iterations. These successive steps were applied until the chi-square functions (mean standard deviation), χ^2, were minimized (less than 0.001). Values of k and n are shown in Table 1.

The average Avrami exponent of 2.1 ± 0.2 (Table 1) indicates that there was initially a homogeneous nucleation of α-alumina followed by a continuous heteronucleation on the grain edges [36]. The nearly constant value of the Avrami exponent, n, for all the isotherms suggests that the kinetics of phase transformation at each temperature under study takes place in a similar mechanism.

γ-Alumina has a spinel cubic lattice with cationic vacancies, as well as anionic vacancies created by removal of water (dehydroxylation) by calcination. The cationic vacancies would diffuse towards the particle surface and the reaction between the cationic and anionic vacancies would destroy the spinel lattice, leading to a structural rearrangement until α-alumina is formed through an exothermic reaction. The annihilation between the vacancies would be the rate-determining step of this mechanism. As a result, α-alumina formation would follow a nucleation and growth mechanism, where homogeneous nucleation occurs in regions rich in anionic or cationic vacancies on the particle surface, while growth proceeds at the reaction interface from the surface through the annihilation reaction between the vacancies [37].

The rate constants for the $\gamma \rightarrow \alpha$-alumina transformation increase with temperature (Table 1), as expected for a thermally activated or Arrhenius processes, since the higher the heating temperature, the shorter the time required for a complete transformation from γ-alumina into α-alumina (Fig. 5). The phase transformation at 900 °C requires less time for the total conversion to α-alumina than the other samples.

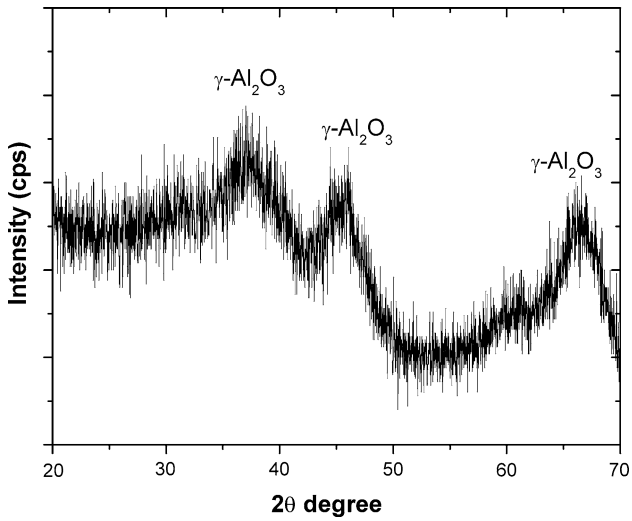

Fig. 3 XRD patterns of the gel heated at 300 °C for 25 min (xerogel)

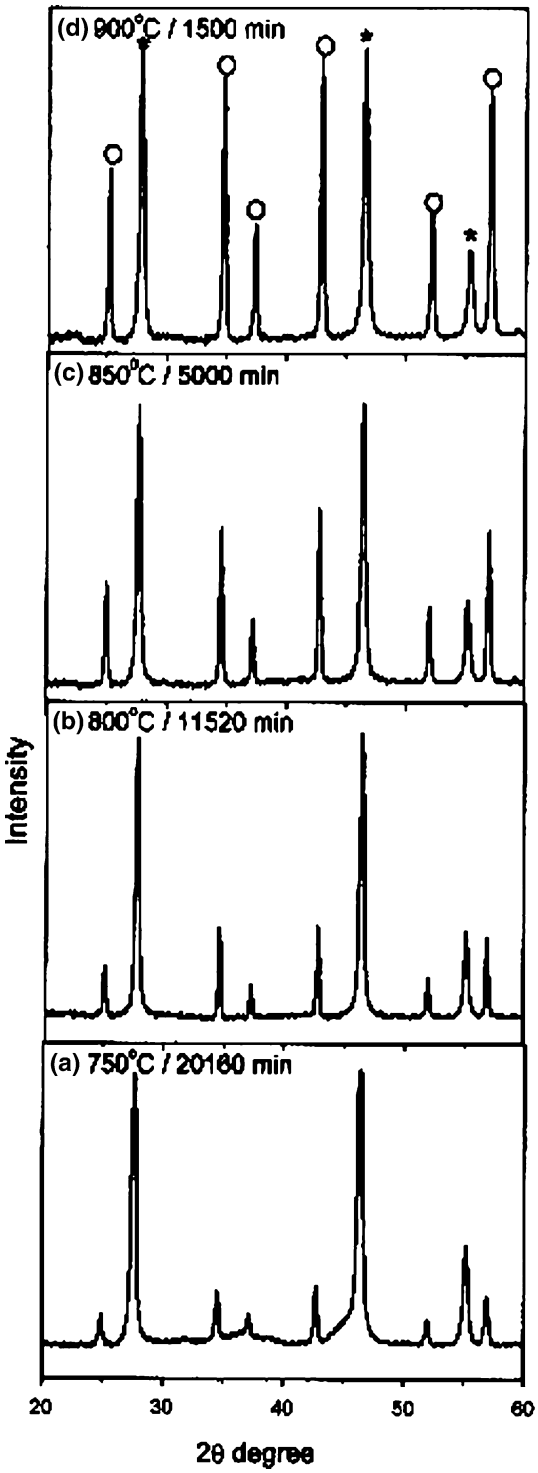

Fig. 4 Quantitative XRD patterns of the xerogel heated at different temperatures for different time periods. (*) CaF_2 and (°) α-alumina

The apparent activation energy for the $\gamma \rightarrow \alpha$-alumina transformation was determined from the isotherms of Fig. 5 through the slope of the Arrhenius plot of In k *versus* $1/T$ (Fig. 6), resulting in the

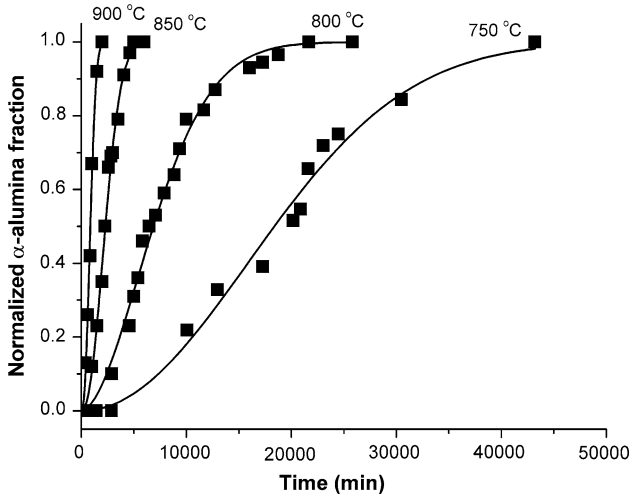

Fig. 5 Isothermal kinetics for the $\gamma \rightarrow \alpha$-alumina phase transformation at the indicated temperatures

Table 1 Rate constants, k, and Avrami exponent, n, at different temperatures

Temperature (°C)	Rate constant (min^{-1})	Avrami exponent
700	$(5.0 \pm 0.1) \times 10^{-5}$	2.1 ± 0.2
800	$(1.20 \pm 0.01) \times 10^{-4}$	1.8 ± 0.1
850	$(3.70 \pm 0.05) \times 10^{-4}$	2.2 ± 0.1
900	$(9.9 \pm 0.3) \times 10^{-4}$	2.4 ± 0.2

apparent activation energy of (201 ± 4) kJ mol^{-1}. This value is lower than those previously reported for the $\gamma \rightarrow \alpha$-alumina transformation [12, 20–23] and can be associated with the higher surface area of the γ-alumina prepared in this work. The low value of the apparent activation energy, a consequence of the high surface area of γ-alumina, can be also related to the kinetic model proposed by Burtin et al. [37]. According to them, the rate of α-alumina formation, dx/dt (where x is the crystallised fraction), is described as a linear function of the initial surface area of the transition alumina. However, their model determines the rate of α-alumina formation in a short surface area range.

In order to verify this kinetic model, we are going to compare the rates of α-alumina formation as a function of the surface areas of the starting materials from Ref. 22, 37 and this work, which corresponds to a wide surface area range. The rates of α-alumina formation published in Ref. 37 were given for the kinetics performed at 1378 K. For comparison with them, data from Ref. 22 and this work were treated in a way that provided simulated kinetics of α-alumina formation at 1378 K, based on Eq. 1 and the apparent activation energy obtained from the Arrhenius plot. Then the

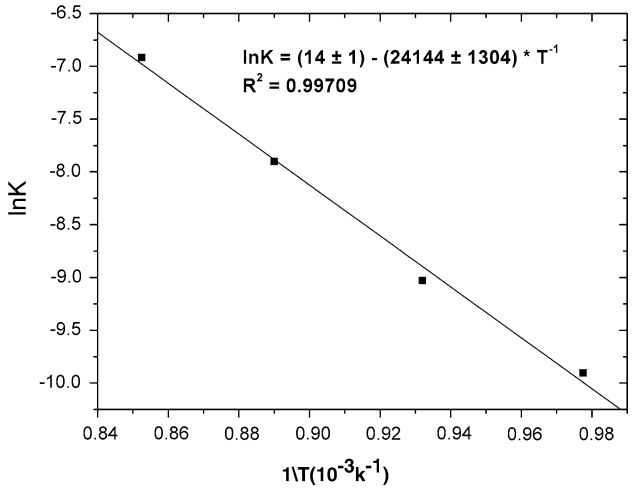

Fig. 6 Arrhenius plot for the $\gamma \rightarrow \alpha$-alumina phase transformation

rates of α-alumina formation, expressed as dx/dt, were determined by the differential function of the α-alumina fraction x and the rate value determined when $x = 0.4$, as done by Burtin et al. in their work [37]. Figure 7 shows the dependence of the rates of α-alumina formation on the surface areas of the starting materials.

Even though the regression of the data from Fig. 7 fairly fits to a straight line, probably due to the errors involved in the dx/dt determination and the wide surface area range, Fig. 7 indicates that the higher the surface area of the starting material, the higher the rate of α-alumina formation, as a consequence of the lower activation energy involved in the $\gamma \rightarrow \alpha$-alumina phase transformation.

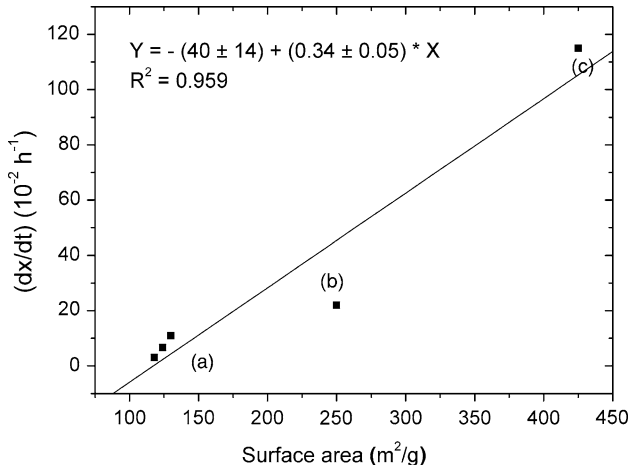

Fig. 7 Rates of α-alumina crystallisation as a function of the surface areas of the starting materials. (**a**) data from Ref. 37. (**b**) value determined from the data reported on Ref. 22. (**c**) value determined in this work

Table 2 $t_{0.75}/t_{0.25}$ ratios and nuclei growth mechanisms [35]

$t_{0.75}/t_{0.25}$ ratio	Nuclei growth mechanism
$1.48 \leq t_{0.75}/t_{0.25} \leq 1.69$	Polyhedral
$1.69 \leq t_{0.75}/t_{0.25} \leq 2.2$	Plate-like
$2.2 \leq t_{0.75}/t_{0.25} \leq 4.82$	Linear

The relation between activation energy and surface area was also verified by Jang et al. [38], who reported that the energy required for the transformation of milled gibbsite to α-alumina (442 kJ mol^{-1}) was lower than that of unmilled gibbsite (481 kJ mol^{-1}).

Thus, the low apparent activation energy involved in the $\gamma \rightarrow \alpha$-alumina phase transformation found in this work, as well as the low α-alumina crystallization temperature of 750 °C, may be related to the high surface area of the γ-alumina, obtained by the sol-gel process.

As stated in the KJMA model, the $t_{0.75}/t_{0.25}$ ratio, where $t_{0.75}$ is the time during isothermal kinetics needed for α-alumina crystallization to reach 75% and $t_{0.25}$ is the time to reach 25%, relates to the nuclei growth mechanisms and differences in the grain morphology.

The average value obtained for $t_{0.75}/t_{0.25}$ from the isotherms (Fig. 5) was (2.1 ± 0.1), which, compared to Table 2, suggest a plate-like growth.

To confirm this result, a SEM micrograph of the xerogel heated at 800 °C for 21,600 min was obtained (Fig. 8). It shows that the α-alumina has a plate-like form, as suggested by the KJMA model.

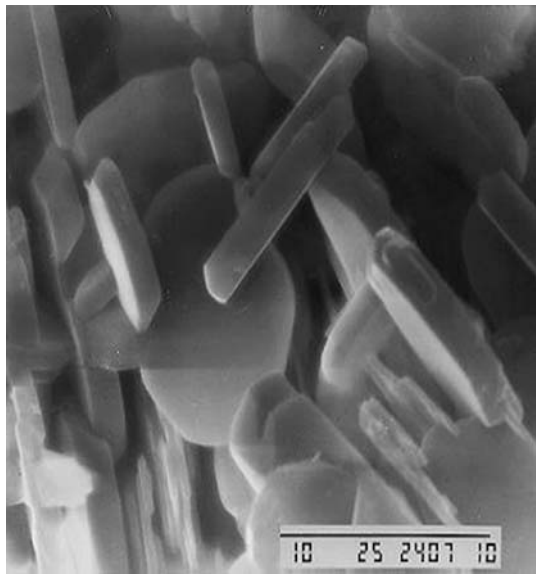

Fig. 8 SEM micrograph for α-alumina crystallised at 800 °C for 21600 min (the bar corresponds to 10 μm)

Conclusions

γ-Alumina was produced by a sol-gel process from a saturated aqueous solution of aluminum nitrate and urea and characterised by ^{27}Al-MAS NMR, FTIR and XRD techniques, as well as the determination of its surface area.

The lower α-alumina crystallization temperature (750 °C), without any intermediate crystalline phases, and apparent activation energy (201 ± 4 kJ mol^{-1}) for the $\gamma \rightarrow \alpha$-alumina phase transformation compared to the values reported until now are consequence of the high surface area (425 m^2/g) of the γ-alumina.

The $\gamma \rightarrow \alpha$-alumina phase transformation was described by a nucleation and growth process, according to the KJMA model. The value of (2.1 ± 0.1) for the $t_{0.75}/t_{0.25}$ ratio corresponded to a plate-like crystallization process, confirmed by the SEM micrograph of the α-alumina.

Acknowledgements The authors would like to thank CNPq and CAPES for financial support.

References

1. Gitzen HW (1970) Alumina as a ceramic material, Am Ceram Soc Columbus, OH pp 84
2. Temuujin J, Jadambaa T, Mackenzie KJD, Angerer P, Porte PF, Riley F (2000) Bull Mater Sci 23:301
3. Sarikaya Y, Ada K, Alemdaroglu T, Bozdogan I (2002) J Eur Ceram Soc 22:1905
4. Llusar M, Pidol L, Roux C, Pozzo JL, Sanchez C (2002) Chem Mater 14:5124
5. Urretavizcaya G, Cavalieri AL, Lopez JMP, Sobrados I, Sanz J (1998) J Mater Synth Process 6:1
6. Sharma PK, Varadan VV, Varadan VK (2003) J Eur Ceram Soc 23:659
7. Nordahl CS, Messing GL (1998) Thermochim Acta 318:187
8. Wefers K, Misra C (1987) Oxides and hydroxides of aluminum, Alcoa Technical Paper No. 19 Rev., ALCOA Labs
9. Stumpf HC, Russell AS, Newsome JW, Tucker CM (1950) Ind Eng Chem 42:1398
10. Lippens BC, Deboer JH (1964) Acta Crystallogr 17:1312
11. Morrissey KJ, Czanderna KK, Carter CB (1984) J Am Ceram Soc 66:C-88
12. Wilson SJ, McConnell JD (1980) J Solid State Chem 34:315
13. Brinker CJ, Scherer GW (1990) Sol-gel science—the physics and chemistry of sol-gel processing. Academic Press, San Diego
14. Saraswati V, Rao GVN, Rao GVR (1987) J Mater Sci 22:2529
15. Assih T, Ayral A, Abenoza M, Phalippou J (1988) J Mater Sci 23:3326
16. Dwivedi RK, Gowda G (1985) J Mater Sci Lett 4:331
17. Pecharroman C, Sobrados I, Iglesias JE, González-Carreño T, Sanz J (1999) J Phys Chem B 103:6160
18. Sohlberg K, Pennycook SJ, Pantelides ST (1999) J Am Ceram Soc 121:7493
19. Ozao R, Ochiai M, Yoshida H, Ichimura Y, Inada T (2001) J Therm Anal Calorim 64:923
20. Shelleman RA, Messing GL, Kumagai M (1986) J Non-Cryst Sol 82:277
21. Nishio T, Fujiki Y (1994) J Mater Sci 29:3408
22. McArdle JL, Messing GL (1993) J Am Ceram Soc 76:214
23. Korunderlieva S, Plachkova B (1993) Interceramics 42:140
24. Macêdo MIF, Osawa CC, Bertran CA (2004) J Sol-Gel Sci Technol 30:135
25. Thim GP, Bertran CA, Barlette VE, Macêdo MIF, Oliveira MAS (2001) J Eur Ceram Soc 21:759
26. Macêdo MIF (1999) Synthesis of alumina by the sol-gel process: kinetics and morphology, PhD thesis, Chemistry Institute, UNICAMP, Campinas
27. Mastikhin VM, Krivoruchko OP, Zolotouskii BP, Buyanou RA (1981) React Kinet Catal Lett 18:117
28. Sanz J, Sobrados I, Cavalieri AL, Pena P, Aza S, Moya JS (1991) J Am Ceram Soc 74:2398
29. Baraton MI, Quintard P (1982) J Mol Struct 79:337
30. Busca G, Lorenzelli V, Ramis G, Willey RJ (1993) Langmuir 9:1492
31. Kolmogorov AE (1937) Bull Acad Sci USSR Mater Sci 1:355
32. Johnson WA, Mehl RE (1939) Trans Am Inst Min Eng 135:416
33. Avrami M (1939) J Chem Phys 20:1103
34. Avrami M (1940) J Chem Phys 8:212
35. Avrami M (1941) J Chem Phys 9:177
36. Put PJV (1998) The inorganic chemistry of materials: how to make things out of elements. Plenum Press, New York
37. Burtin O, Brunelle JP, Pijolat M, Soustelle M (1987) Appl Catal 34:239
38. Jang SW, Lee HY, Shin KC, Lee SM (2001) J Ceram Process Res 2:67